ISSN 2072-5981
doi: 10.26907/mrsej

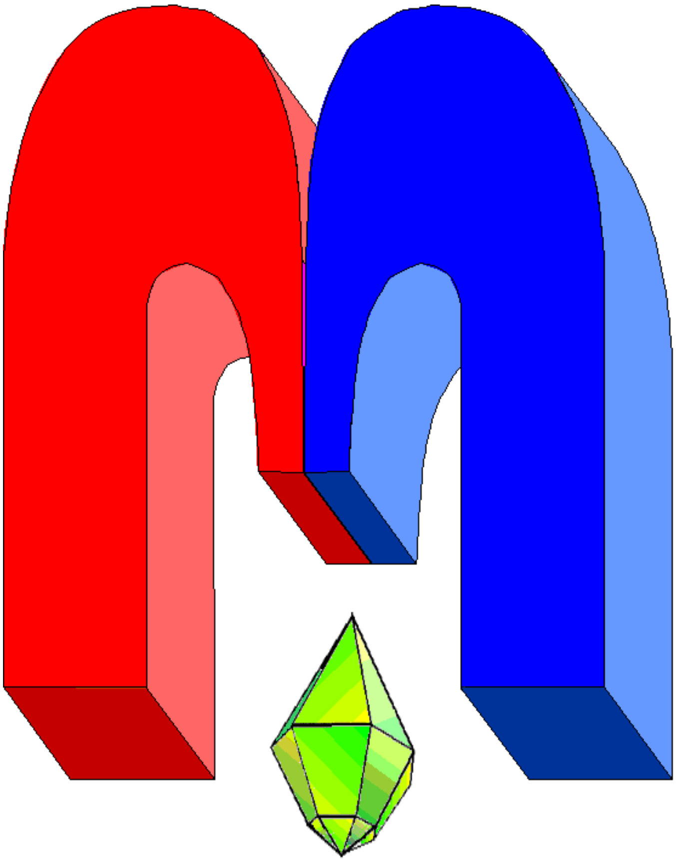

Magnetic Resonance in Solids

Electronic Journal

Volume ***21***
Issue ***1***
Paper No ***19105***
1-7 pages
2019
doi: **10.26907/mrsej-19105**

http://mrsej.kpfu.ru
http://mrsej.ksu.ru

Established and published by Kazan University
Endorsed by International Society of Magnetic Resonance (ISMAR)
Registered by Russian Federation Committee on Press (#015140),
August 2, 1996
First Issue appeared on July 25, 1997

"***Magnetic Resonance in Solids. Electronic Journal***" (**MRSej**) is a peer-reviewed, all electronic journal, publishing articles which meet the highest standards of scientific quality in the field of basic research of a magnetic resonance in solids and related phenomena.

Indexed and abstracted by
Web of Science (*ESCI*, Clarivate Analytics, from 2015),
Scopus (Elsevier, from 2012), *RusIndexSC* (*eLibrary*, from 2006), *Google Scholar*,
DOAJ, *ROAD*, *CyberLeninka* (from 2006), *SCImago Journal & Country Rank*, etc.

---

* In Kazan University the Electron Paramagnetic Resonance (EPR) was discovered by Zavoisky E.K. in 1944.

Short cite this: *Magn. Reson. Solids* **21**, 19105 (2019) doi: 10.26907/mrsej-19105

Study of radiation-induced stable radicals in synthetic octacalcium phosphate by pulsed EPR[†]

D. Shurtakova [1,*], B. Yavkin [1,2], M. Gafurov [1], G. Mamin [1], S. Orlinskii [1], L. Kuznetsova [3], S. Bakhteev [4], I. Ignatyev [5], I. Smirnov [6], A. Fedotov [6], V. Komlev [6]
[1] Kazan Federal University, Kremlevskaya 18, Kazan 420008, Russia
[2] Physikalisches Institut, University of Stuttgart, Pfaffenwaldring 57, Stuttgart 70569, Germany
[3] Kazan State University of Architecture and Engineering, Zelenaya 1, Kazan 420043, Russia
[4] Kazan National Research Technological University, K. Marx Str. 41, Kazan 420015, Russia
[5] Interregional Clinical Diagnostic Centre, Karbysheva 12a, Kazan 420101, Russia
[6] A.A. Baikov Institute of Metallurgy and Materials Science, Russian Academy of Sciences, Leninsky Pr. 49, Moscow 119991, Russia
**E-mail: darja-shurtakva@mail.ru*

(Received December 18, 2018; accepted December 19, 2018; published January 30, 2019)

Created at room temperature by X-ray irradiation at the dose of about 5 kGy radiation-induced centers in stable octacalcium phosphate (OCP) powders obtained by double transformation of α-tricalcium phosphate (TCP) are studied by means of pulsed electron paramagnetic resonance (EPR). No EPR signals within the sensitivity of the used equipment in the non-irradiated samples were detected. In the irradiated species complex EPR spectrum signals appeared. Three types of the paramagnetic centers are decomposed in the investigated samples. Their spectroscopic parameters (components of *g*-factors and hyperfine constants) are defined. Based on the extracted parameters two of them are ascribed to CO_2^- and NO_3^{2-} radicals while the nature of the third one is still questionable. The spectroscopic parameters of NO_3^{2-} stable radical is found to be differ than these for TCP or hydroxyapatite. The obtained results could be used for the tracing of the mineralization processes from its initiation to the completion of the final product and for the identification of the OCP phase.

PACS: 75.10.Dg, 76.30.-v, 75.20.

Keywords: calcium phosphate, octacalcium phosphate, EPR, radiation-induced paramagnetic centers.

1. Introduction

Processes of biomineralization and s attract scientific attention during a long time [1]. The fact that complete bone tissue forms within atherosclerotic artery wall has been already known since at least the 1800s. Vascular calcification was recognized as an osteogenic process that is an essential part of coronary atherosclerosis (AS). However, for most of the 20th century, vascular calcification has been considered to be a passive degenerative process occurring at the end stage of atherosclerotic plaque (ASP) formation, because the paradigm for pathogenesis of atherosclerosis shifted towards "lipid hypothesis" that high blood cholesterol levels contribute causally to AS and ASP growth. Only over the last two decades vascular calcification has been increasingly recognized as an active, organized, regulated and preventable process with remarkable similarities to bone formation [2].

Recent investigations [3-5] and earlier works [6, 7] have shown that the mineral of cardiovascular pathological deposits consists of poorly crystalline, non-stoichiometric carbonate substituted calcium phosphates (CaP) similar (in its matured stage) to the hydroxyapatite (HA, chemical formula $Ca_{10}(PO_4)_6(OH)_2$). Synthetic CaPs are also in the focus of the modern material science and technology as the most suitable matrix for tissue (first of all for bone and dental) engineering [8, 9], including myocardial tissue regeneration [10]. However, neither a functional role nor the sites of predominant location of excessive calcium in pathological mineral deposits with apatite-like structure are clear while the nature of the precursor phase during the biomineralization process is still

---

[†] This paper was selected at XX International Youth Scientific School "Actual problems of magnetic resonance and its application", Kazan, 24–29 September 2018. The MRSej Editors, Prof. M.S. Tagirov and Prof. V.A. Zhikharev, are responsible for the publication.

controversial [11-13]. It forces to apply new or modify the known analytical tools for the characterization and investigations of model (synthetic) and real (synthetic and of biogenic origin) CaPs.

Among the analytical, non-destructive tools for CaPs investigations both of biogenic and synthetic origins is electron paramagnetic resonance (EPR) [14-16]. Though the attempts to apply EPR for ASP investigations are known since 1970s [17-19], the increased sensitivity, spectral and temporal resolution along with the improved stability of the commercial EPR spectrometers opened new possibilities in the CaP studies last decade [15, 16] making a step towards in-situ EPR imaging (EPRI) [20].

Several inorganic phases involved into the biomineralization processes being hypothesized. They include (besides of HA) tricalcium phosphate (TCP, chemical formula Ca_3PO_4), dicalcium phosphate dihydrate (DCPD, $CaHPO_4 \cdot 2H_2O$, brushite), octacalcium phosphate (OCP, $Ca_8H_2(PO_4)_6 \cdot 5H_2O$). Various studies suggested that OCP is the direct precursor phase of biogenic HA (see [11] and references therein) since the results of in vitro (in simulated body fluid) crystal growth studies. Therefore, OCP offers also a fascinating alternative as a transient intermediate to the biogenic apatite for bone regeneration. Similar to HA, the structural properties of OCP can be changed by many methods, e.g. ion substitution. Thus, the physicochemical characteristics of OCP have to be extensively investigated with a view to enhancing its properties.

Pure, non-substituted OCP (as well as the mentioned HA and TCP) is EPR silent. Consequently, conventional EPR can be used for the purity check of OCP materials in sense of the presence of metal impurities, for example [15, 16, 21]. A conventional way for studying EPR silent CaPs is a creation and investigation of influence of the ionizing radiation like X-, β-, γ-rays, ultraviolet, etc. Several radiation-induced paramagnetic species (anion radicals) located at hydroxy or phosphate sites have been identified in synthetic HA: oxygen radical O^-, trapped atomic hydrogen, and hole trapped on OH^- and PO_4^{2-}. Carbonate radicals CO_2^-, CO_3^-, and CO_3^{3-} are often observed as well as additional organic radicals (alanine-like) signals and color centers signals appears. In burnt bones the coal-type C• radicals were identified [22, 23]. In HA synthesized by the solid state phase methods or wet-synthesis technique from the nitrate containing substances stable H^0 and / or NO_3^{2-} radicals, correspondingly, are often detected [14, 23].

In this paper we investigate radiation-induced defects in OCP. To the knowledge of the authors, the only OCP related studies of the radiation-induced paramagnetic centers are the papers [24, 25] in which carbonated apatites were obtained by the hydrolysis of OCP in Na_2CO_3 solutions. In ref. [26] we presented preliminary results of our study of the X-ray created paramagnetic centers in OCP.

2. Materials and Methods

Synthesis of α-TCP was carried out by precipitation from solutions of calcium nitrate and ammonium hydrogen phosphate:

$$3Ca(NO_3)_2 + 2(NH_4)_2HPO_4 + 2NH_4OH \rightarrow Ca_3(PO_4)_2 + 6NH_4NO_3 + 2H_2O. \quad (1)$$

A solution of ammonium hydrogen phosphate (0.5 mol/L) was gradually added to a solution of calcium nitrate (0.5 mol/L) with constant stirring. The resulting suspension was allowed to age in the air during the 3 hours. The precipitate was then filtered off and dried at 80°C. For the production of α-TCP ceramic granules, the technology of impregnating a cellular polymeric template with ceramic slip was used [27], followed by sintering at 1300°C with quenching. The quenching was carried out by cooling the ceramics at room temperature. After that, the ceramic was crushed and granules of 500-1000 μm were sifted.

Ceramic granules of α-TCP were transformed to OCP according to the route described in ref. [28]. Briefly, 10 g of α-TCP ceramic granules were immersed to 1000 mL of 1.5 M sodium acetate aqueous solution and 0.15 ± 0.02 M glutamic amino acid, adjusted with orthophosphoric acid to a pH value of 5.5 ± 0.1. The granules were kept in for 168 h with shaking at 35°C, then thoroughly washed in distilled water five times and dried overnight at 37°C. Then, the granules were immersed in an aqueous 1.5 M sodium acetate solution with a pH value of 8.7 ± 0.1 for 168 h with shaking at 35°C.

The phase composition was determined by powder X-ray diffraction (XRD) technique (Shimadzu XRD-6000 (Japan), Ni-filtered CuKα1 target, $\lambda = 1.54183$ Å. Samples were scanned from $2\Theta = 3°$ to 40° with a step of 0.02°. The XRD pattern of the product obtained after soaking in standard buffer solution for 168 h is shown in Figure 1. XRD of the investigated samples confirmed OCP phase with following characteristic: (010) main reflection at $2\Theta = 4.9°$ and peaks (260), (151) and (150), (070), (002).

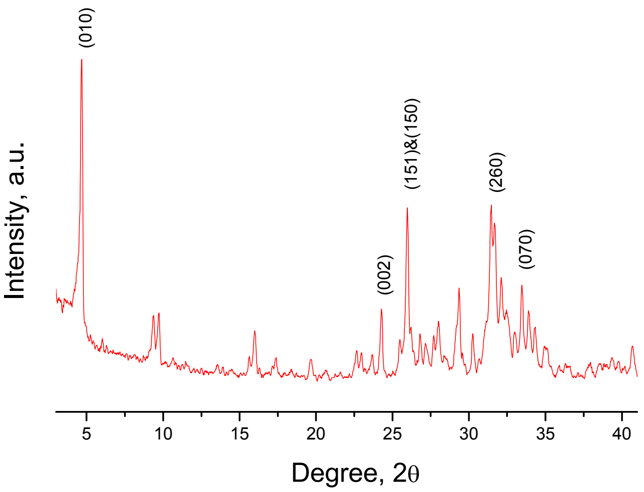

Figure 1. XRD pattern of the OCP powder sample.

The crystal structure of OCP is triclinic with a space group of $P\bar{1}$ (the center of inversion is located at (½, ½, ½), the unit cell contains 110 atoms) and exhibits the much longer *a* axis dimension than the *b*. OCP has the lattice constants $a \approx 19.8$ Å, $b \approx 9.6$ Å, $c \approx 6.87$ Å, $\alpha \approx \beta \approx 90°$ and $\gamma \approx 109°$. As it was already mentioned in Introduction, it resembles the structure of hydroxyapatite with the corresponding hydroxyapatite constants for $P6_3/m$ hexagonal group $a = b \approx 9.42$ Å, $c \approx 6.885$ Å, $\alpha = \beta \approx 90°$ and $\gamma \approx 120°$ [29]. In ref. [30] it was first shown that OCP consists of apatite and hydrated layers. It has been suggested that a progressive evolution from OCP to apatite can occur by a topotactic reaction corresponding to the elimination of the hydrated layer. For the clarity, crystal structure of OCP compared to the HA structure schematically presented in Figure 2.

There are eight kinds of Ca sites and six kinds of P sites forming PO_4 tetrahedra. Often is assumed that two kinds of PO_4 tetrahedra (centered at P-5 and P-6) are in the form of HPO_4 because of hydrogen attachment. For comparison, in the HA crystal structure there are only two sites for calcium ions, while anionic substitution can occur to two different sites (OH and PO_4). In TCP structure five different calcium positions and three PO_4 positions are distinguished. The existence of differently coordinated calcium sites for cationic and up to six phosphorous sites for the anionic replacement in the crystal structure of OCP crystal structure brings more possibilities of complex ionic substitution and makes, therefore, ion substituted OCP much harder for the theoretical and experimental investigations.

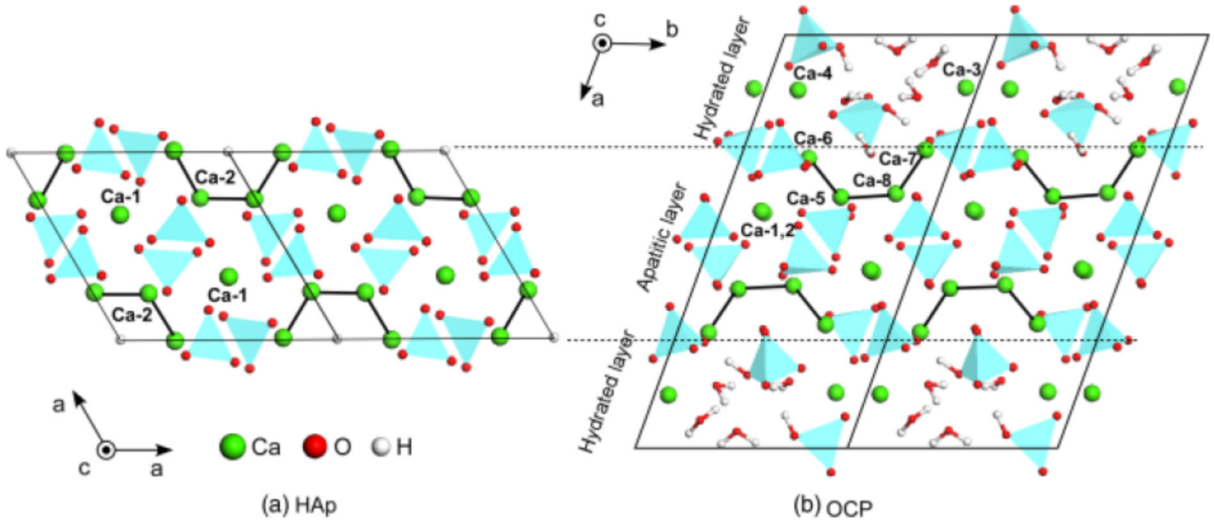

(a) HAp

(b) OCP

Figure 2. Crystal structures of Hap (left panel) and OCP (right panel) viewed along the c axis. PO_4 groups involved are represented by blue tetrahedral (adapted from [29]).

The chemical content of the powders was defined by the X-ray fluorescence analysis with total external reflection (S2 Picofox, Bruker) at room temperature that (within the limit of sensitivity) affirms the composition of the investigated species and absence of other impurities.

Conventional (continuous wave, CW) and pulsed EPR measurements were done exploiting the abilities of Bruker Elexsys 580 spectrometer. X-ray irradiation of the synthesized powders was provided by using URS-55 source ($U = 55$ kV, $I = 16$ mA, W anticathode) at room temperature with the estimated dose of 5 kGy to create stable paramagnetic centers in the nominal pure material. Typically, electron spin echo (ESE) experiments were done by using 2 pulse Hahn echo scheme $\pi/2$-τ-π-τ-ESE with $\pi = 32$ ns and $\tau = 240$ ns.

3. Results and Discussion

In all investigated samples no EPR signal was detected at room temperature (i.e. concentration of the paramagnetic impurities $C < 10^{13}$ spin/g) while after the irradiation a signal in the central part of the spectrum appears with the total concentration of $C \approx 8(1)\cdot 10^{16}$ spin/g (Figure 3). Both CW and 2-pulse Hahn electron-spin-echo (ESE) were detected at RT. Their comparison is presented in Figure 3 which shows that the chosen EPR detection parameters do not influence the presented results.

In paper [26] the dependence of the CW spectrum on microwave power in pure OCP was shown. At least two different sorts of paramagnetic centers could be distinguished in the investigated species: while the intensity and amplitude of the broad line in the middle of the spectrum with the linewidth of about 2 mT (which is denoted as R_3 radical, see text below) is growing with power, the second “structural” paramagnetic centre (R_1) with the maximal splitting of 5 mT starts to saturate already at $P_{MW} = 10$ mW. Study of the electronic spin-lattice relaxation times T_{1e} curves obtained by saturation-recovery measurements at the maximum of ESE signal (position B_1 in Figure 3) shows that T_{1e} curves could be properly fitted only as a sum of three exponents with $T_1^{(1)} = 0.02$ ms, $T_1^{(2)} = 0.2$ ms, $T_1^{(3)} = 1.2$ ms (Figure 4).

Based on the experience gathered by characterization of radiation-induced defects in hydroxyapatite [31] and assuming the existence of three types of stable paramagnetic centers, we have analyzed the ESE spectra by using the abilities of Easyspin for Matlab program [32]. The results are presented in Figure 5, the values of corresponding EPR parameters are listed in Table 1.

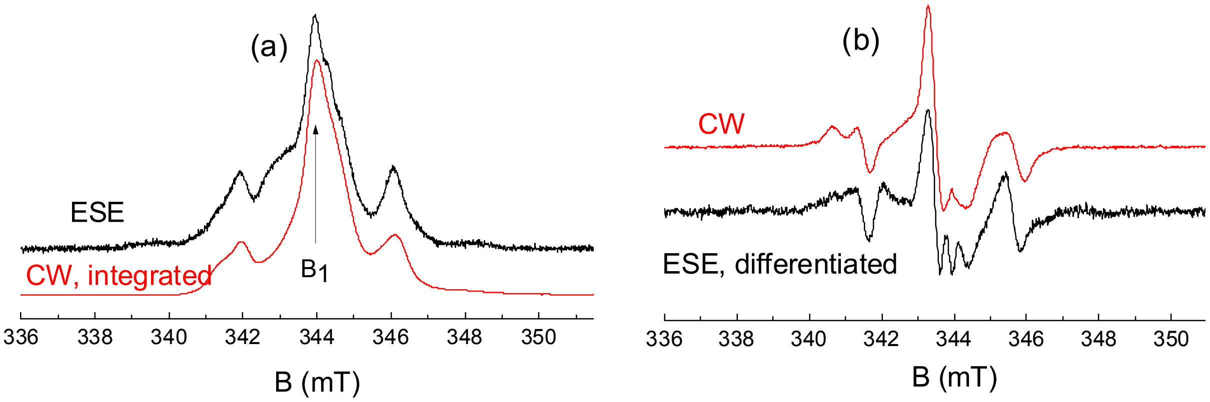

Figure 3. Comparison of CW and ESE detected EPR of OCP sample. Magnetic field value (B_1) for which the electronic relaxation times were measured is marked.

Table 1. EPR parameters for the stable radical centers used for the simulation of the registered EPR spectrum.

Radical	Possible origin	$g_{\parallel}$	$g_{\perp}$	$A_{\parallel}$ (mT)	$A_{\perp}$ (mT)	$\Delta H_{1/2}$ (mT)
R_1	NO_3^{2-}	2.0055(5)	2.0036(5)	3.05(5)	2.006(4)	–
R_2	CO_2^-	1.9976(5)	2.0032(4)	–	–	–
R_3	–	2.0045(5)	2.0045(5)	–	–	2.53

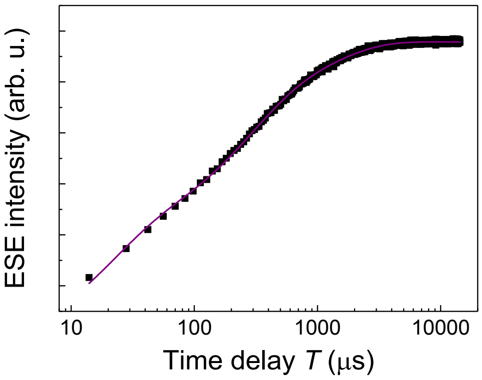

Figure 4. T_1 curve (filled squares) and its corresponding fitting with three exponents at $T = 100$ K.

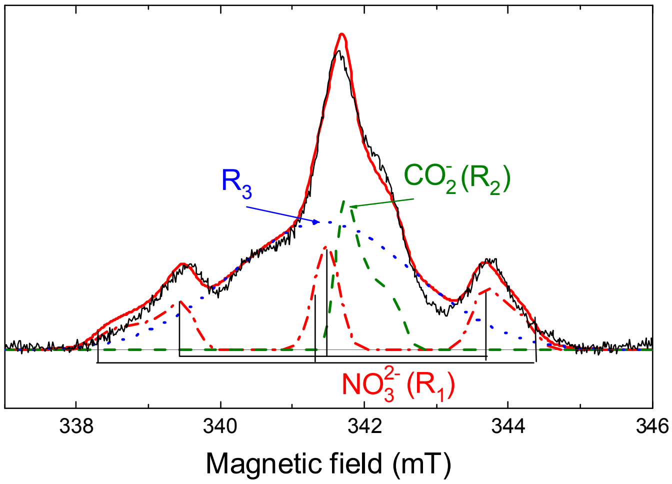

Figure 5. ESE spectra at RT along with the fitting as a sum of three signals.

It is known that paramagnetism in apatites is mainly due to the oxygen-containing radicals (see section Introduction). In the most cases the powder EPR spectra for these radicals can described by the spin-Hamiltonian of the axial symmetry:

$$H = g_{\parallel}\beta B_z S_z + g_{\perp}\beta\left(B_x S_x + B_y S_y\right) + A_{\parallel} S_z I_z + A_{\perp}\left(S_x I_x + S_y I_y\right), \tag{1}$$

where $g_{\parallel}$ and $g_{\perp}$ are the main components of the g tensor, $A_{\parallel}$ and $A_{\perp}$ are the main components of the hyperfine tensor, B_i, S_i and I_i are the projections of the external magnetic field strength, $S = ½$ and $I = 1$ are electronic and nuclear spin correspondingly onto the $i = \{x, y, z\}$ coordinate axis, β is a Bohr magneton.

R_1 radical could be ascribed to the nitrogen containing species due to $I = 1$ for ^{14}N nuclei. The obtained for R_1 radical values are less than those for the well-studied (also by our group) hydroxyapatite [33]. The HA spectra could be simulated properly with $A_{\parallel} = 6.65(40)$ mT and a discrete distribution of $A_{\perp}$ around 3.37(5) mT, while the components of g-factors for all of the obtained radical's modifications are the same: $g_{\parallel} = 2.0011(1)$, $g_{\perp} = 2.0052(1)$. It was concluded that in the irradiated HA samples EPR is mainly due to the stable NO_3^{2-} ions preferably substituting one of the PO_4^{3-} position in the HA structure (substitution of B-type). In our paper [9] we reported that EPR spectrum of the wet synthesized TCP after radiation is also mainly due to the NO_3^{2-} with the same as for HA value of $A_{\parallel}$ but the distribution of $A_{\perp}$ (A_2, A_3) is larger than that for the HA. We have suggested that it could be due to the three different positions for PO_4 group substitution in TCP structure as well as due to the various schemes of the charge compensation.

As it follows from the presented results, in OCP it could be suggested that other nitrogen containing radicals such as NO_2 for example [33] or located in other than apatite PO_4^{3-} position are preferable. We hope our planned ENDOR experiments could help to unravel the nature of the R_1 radical.

The values of g-components for R_2 radical are the sign of the apatite CO_2^- stable radical of axial symmetry [23]. It is known that this type of radicals can substitute not only B site but also OH^- (A site) in apatite structure. The axial symmetry of the g-tensor of the species observed in the A-type carbonated apatite EPR spectrum is due to the radical rotation about the g_y direction while the shapes and widths of the lines in the ESR spectra of the species in A-type carbonated apatites strongly depend on the method of sample preparation.

The nature of the broad line at $g = 2.0045$ is still unclear. It may be connected with the ozonide complexes adsorbed on the OCP crystal surface (or interphase surface) and, especially, with the various types of CO_3^{3-} radicals which lines are situated in the range 2.0030-2.0047 [23]. We hope that a series of differently synthesized OCP species would allow to shed light on the nature of the observed signal.

4. Summary

In spite of decades of investigation, the nature and location of stable radiation-induced paramagnetic centers in natural and even synthetic apatites is still a matter of discussions. Mainly the hydroxyl and fluorapatites as the mimicking the natural materials of biogenic origins are studied. Presence and diversity of the obtained paramagnetic species strongly depends on the synthesis route and corresponding treatment. From one side it hinders the application of the radiation-induced centers for dating purposes and as sensitive probes in biomedical research. From other side it gives a key to follow the biochemical processes and calcium phosphate transformations. We hope that our investigation of OCP is one more step in this direction.

Acknowledgments

This work was supported by Russian Foundation for Basic Research (RFBR), grant # 18-29-11086.

References

1. Blankenhorn D.H. *Am. J. Med. Sci.* **242**, 41 (1961)
2. Shioi A., Ikari Y. *J. Atheroscler Thromb.* **25**, 294 (2018)
3. Danilchenko S.N., Kalinkevich A.N., Moskalenko R.A., Kuznetsov V.N., Kochenko A.V., Husak E.V., Starikov V.V., Liu F., Junhu M., Lü J. *Interv. Med. Appl. Sci.* **10**, 110 (2018)
4. Cottignoli V., Relucenti M., Agrosì G., Cavarretta E., Familiari G., Salvador L., Maras A. *BioMed Res. Int.* **2015**, 542687 (2015)
5. Usachev K., Mamin G., Gafurov M., Ignat'ev I., Kamaltdinov R., Salakhov M., Murzakhanov F., Kiiamov A., Osin Y., Chelyshev Y., Orlinskii S. *Eur. J. Clin. Invest.* **48**, 137 (2018)
6. Gilinskaya L.G., Grigorieva T.N., Okuneva G.N., Vlasov Y.A. *J. Struct. Chem.* **44**, 622 (2003)
7. Becker A., Epple M., Müller K.M., Schmitz I.A. *J. Inorg. Biochem.* **98**, 2032 (2004)
8. Habraken W., Habibovic P., Epple M., Bohner M. *Materials Today* **19**, 69 (2016)
9. Fadeeva I.V., Gafurov M.R., Kiiaeva I.A., Orlinskii S.B., Kuznetsova L.M., Filippov Y.Y., Fomin A.S., Davydova G.A., Selezneva I.I., Barinov S.M. *BioNanoScience* **7**, 434 (2017)
10. Silvestri A., Boffito M., Sartori S., Ciardelli G. *Macromol. Biosci.* **13**, 984 (2013)
11. Rau J.V., Fosca M., Komlev V.S., Fadeeva I.V., Rossi Albertini V., Barinov S.M. *Crys. Growth Des.* **10**, 3824 (2010)
12. Curtze S.C., Kratz M., Steinert M., Vogt S. *Sci. Rep.* **6**, 23285 (2016)
13. Srinivasan A., Ramaswamy V., Kuruvilla S., Sehgal P.K., Balakrishnan K. *Ind. J. Thorac Cardiovasc. Surg.* **28**, 6 (2012)
14. Abdul'yanov V.A., Galiullina L.F., Galyavich A., Izotov V.G., Mamin G.V., Orlinskii S.B., Rodionov A.A., Salakhov M.K., Silkin N.I., Sitdikova L.M., Khairullin R.N., Chelyshev Y.A. *JETP Lett.* **88**, 69 (2008)
15. Chelyshev Y., Gafurov M., Ignatyev I., Zanochkin A., Mamin G., Sorokin B., Sorokina A., Lyapkalo N., Gizatullina N., Mukhamedshina Y., Orlinskii S. *BioMed Res. Int.* **2016**, 3706280 (2016)
16. Gabbasov B., Gafurov M., Starshova A., Shurtakova D., Murzakhanov F., Mamin G.,Orlinskii S. *J. Magn. Magn. Mater.* **470**, 109 (2019)
17. Ostrowski K., Dziedzic-Gocławska A., Stachowicz W., Michalik J. *Histochem. Cell Biol.* **32**, 343 (1972)
18. Gilinskaya L.G., Okuneva G.N., Vlasov Y.A. *J. Struct. Chem.* **44**, 813 (2003)
19. Stadler N, Lindner R.A., Davies M.J. *Arterioscler. Thromb. Vasc. Biol.* **24**, 949 (2004)
20. Gustafsson H., Hallbeck M., Lindgren M., Kolbun N., Jonson M., Engström M., de Muinck E., Zachrisson H. *Magn. Reson. Med.* **73**, 1682 (2015)

21. Murzakhanov F., Gabbasov B., Iskhakova K., Voloshin A., Mamin G, Putlyaev V., Klimashina E., Fadeeva I., Fomin A., Barinov S., Biktagirov T., Orlinskii S., Gafurov M. *Magn. Reson. Solids* **19**, 17207 (2017)
22. Wencka M., Hoffmann S., Hercman H. *Acta Physica Polonica A* **108**, 331 (2005)
23. Fattibene P., Callens F. *Appl. Radiat. Isot.* **68**, 2033 (2010)
24. Moens P.D.W., Callens F.J., Matthys P.F.A., Boesman E.R., Verbeeck R.M.H. *Appl. Magn. Reson.* **6**, 121 (1994)
25. Doorslaer S., Moens P., Callens F. *Appl. Magn. Reson.* **10**, 87 (1996)
26. Gafurov M., Yavkin B., Mamin G., Orlinskii S., Smirnov I., Fedotov A., Komlev V.S. *IOP Conf. Ser. Earth Environ. Sci*. **155**, 012018 (2018)
27. Fedotov A, Bakunova N., Komlev V., Barinov S. *Doklady Chem.* **439**, 233 (2011)
28. Komlev V., Barinov S., Bozo I., Deev R.V., Eremin I., Fedotov A., Gurin A., Khromova N., Kopnin P., Kuvshinova E., Mamonov V., Rybko V., Serggeva N., Teterina A., Zorin V. *ACS Appl. Mater. Interfaces* **6**, 16610 (2014)
29. Matsunaga K. *J. Am. Ceram. Soc.* **93**, 1 (2010)
30. Brown W. *Nature* **196**, 1048 (1962)
31. Biktagirov T., Gafurov M., Mamin G., Klimashina E., Putlayev V., Orlinskii S. *J. Phys. Chem. A* **118**, 1519 (2014)
32. Stoll S., Schweiger A. *J. Magn. Reson.* **178**, 42 (2006)
33. Gafurov M., Biktagirov T., Mamin G., Orlinskii S. *Appl. Magn. Reson.* **45**, 1189 (2014)